Early warning of shallow landslides: monitoring of pre-failure suction-induced deformation

Lucia Coppola[1#], *Alfredo* Reder[2], *Alessandro* Tarantino[3], *Giovanni* Mannara[4], *Luca* Pagano[1]

[1]*Dipartimento di Ingegneria Civile, Edile e Ambientale, Università di Napoli Federico II, Italy*
[2] *REgional Model and geo-Hydrological Impacts-REMHI, Centro Euro-Mediterraneo sui Cambiamenti Climatici, Italy*
[3] *University of Strathclyde, Scotland, UK*
[4] *IVM srl, Castellammare di Stabia, Italy*
[#]*Corresponding author: lucia.coppola@unina.it*

ABSTRACT

Most of the Landslides Early Warning Systems (LEWS) in operation are based uniquely on monitoring rainfall data, limiting their performance due to false alarms generated by rainfall thresholds. The accuracy of LEWS may be remarkably improved by monitoring soil-based variables and the stress-strain response of the ground during intense rainfall events. This paper investigates whether slope pre-failure deformation can be used as an additional precursor of landslide triggering. This further precursor would substantially improve LEWS accuracy, especially if pre-failure deformation is combined with suction monitoring. Some tests were conducted using a small-scale physical model of a slope built with unsaturated volcanic silt subjected to artificial rainfall. A new device named tensio-Inclinometer was developed to monitor simultaneously suction and suction-induced deformation. It combines a conventional tensiometer and an accelerometer installed at the top of the tensiometer shaft. It is shown that pre-failure deformation detected by the tensiometer shaft tilting is a suitable landslide precursor. Moreover, it can provide reliable soil-based thresholds for early warning systems if combined with suction.

Keywords: Shallow landslides; soil suction; tilting; slope pre-failure deformation.

1. Introduction

During recent decades, rainfall-induced shallow landslides in coarse-grained volcanic fall deposits evolved into debris flows, causing significant damages and fatalities worldwide. Volcanic fall deposits are typically in a partially saturated state, which generates high suction values able to determine high porosity values. Rainwater infiltration causes a drop in suction, and due to high porosity, this class of materials is susceptible to generating fast-moving debris flows.

The risk reduction strategy for this class of landslides is based on Landslide Early Warning Systems (LEWS). Due to the rapidity of the sliding mass movement, alarms must be issued well ahead of the landslide trigger (UNISDR, 2006; Alfieri et al., 2012; Greco & Pagano, 2017). LEWS need to be based on specific landslide precursors. Their performance depends directly on the precursor variables to be monitored, and the model used to set alarm thresholds.

Rainfall is considered the main and often the only precursor variable in most of the LEWS currently in operation (e.g. Keefer et al., 1987; Ortigao and Justi, 2001; Chleborad et al., 2008; Baum et al., 2008; Baum & Godt, 2010; Pagano et al., 2010; Formetta et al., 2016; Pecoraro et al., 2019). However, the low accuracy of such a kind of LEWS leads to setting a conservative alarm threshold, increasing the number of potential false alarms (Greco & Pagano, 2017; Intrieri et al., 2012; Sattele et al., 2015; Reder & Rianna, 2021). A step forward in enhancing the performance of LEWS could be obtained by including some precursor variables. Most of the previous studies consider volumetric water content as an additional precursor variable because the variation of volumetric water content is an indicator of loss of suction and, hence, shear strength (Orense et al., 2003; 2004; Baum et al., 2010; Ponziani et al., 2012; Thiebes et al., 2014; Uchimura et al., 2015; Segoni et al., 2018). However, volumetric water content is not a suitable landslide precursor as pore-water pressures triggering slope failures are generally in the range of a few kilopascals, either in the negative or positive range (Balzano et al., 2019 a,b). In this interval, volumetric water content is characterised by poor sensitivity in the negative range of pore-water pressures (the water retention curve tends to level off when approaching saturated conditions) and no sensitivity in the positive range of pore-water pressures.

This paper investigates whether suction and suction-induced pre-failure deformation can be used as landslide precursors. Shallow slope failure in silty/sandy soils typically happens with a clear failure surface as detected ex-post (Balzano et al., 2019 a,b). The failure initiation is characterised by relatively large displacements of the mass above the failure surface generated by very high shear deformations near the failure surface (shear band). This stage can be preceded by diffuse shear and compressive plastic deformations above the failure surface, referred to as 'pre-failure suction-induced deformations' in this work. Combining pre-failure

deformation with suction monitoring would potentially lead to substantial improvement in LEWS accuracy.

A slope physical model was used to test whether substantial pre-failure deformations occur before wetting-induced instability. First, the slope was reconstituted using natural volcanic soil and reproducing the porosity and the slope inclination typical of the field (Balzano et al. 2019b). The layer is then tilted and subjected to artificial rainfall until failure. Finally, soil suction and slope deformation were monitored using a tensio-inclinometer purposely developed for this research (Coppola et al., 2022) and designed to be later used in the field to underpin real LEWS. Although the experiments presented in this paper focus on volcanic soils, the results are expected to be extended to the broader class of coarse-grained silty materials.

First, the paper describes the tensio-inclinometer, then the setup of the experimental activity, and finally results are discussed.

2. The tensio-inclinometer

The tensio-inclinometer connects a conventional tensiometer measuring pore-water pressure in negative and positive ranges and an accelerometer, installed at the top of the tensiometer shaft, to measure its inclination as a suitable proxy measurement of landslide pre-failure deformation (Fig. 1).

Pore-water pressure appears to be a more effective precursor than volumetric water content. Silty volcanic slopes are typically cohesionless and characterised by inclinations close to the friction angle. So, pore-water pressures triggering slope failures occur in the range of a few kilopascals, in the negative or positive range. Tensiometers show an accuracy of about 1 kPa and can measure pore-water pressure in both negative and positive ranges. These features make tensiometers employment a better precursor of rainfall-induced shallow landslides.

Some studies generally monitor surface displacements using total station, Global Positioning System (GPS) and photogrammetric techniques (Barla & Antolini, 2016; Zhu et al., 2017). However, adverse weather conditions can remarkably reduce visibility during rain events and affect the quality of photographic images.

The accelerometer used for measuring tensiometer shaft inclination was included in a metal box, in turn, clamped to the shaft via a clamping hook to be easily removed for maintenance or replacement. The metal box was designed to retrofit every commercial tensiometer.

The tensio-inclinometer was designed to operate wirelessly. Specifically, a battery supplied power while the recorded data was transmitted using a WI-FI system. The electronics required for pore-water pressure, tilting measurement, data storage, and data transmission are installed on a semiconductor chip. The battery and the semiconductor chip are in the metal box (Fig. 1).

The tensio-inclinometer design ensures rapidity of installation and/or replacement and avoids malfunctioning due to cable damage by wild animals. Furthermore, the wireless monitoring of two precursor variables in a single element is more advisable than approaches based on different elements connected by cables (e.g. Yang et al., 2017).

The tensiometer (T4, UMS GmbH, Munich, Germany) is made up of an acrylic-glass shaft (of variable length in-between 0.15-2 m), developed to monitor pore-water pressure in the range from - 85 kPa to 100 kPa. A high air-entry value saturated ceramic cup is situated at the bottom of the shaft to allow water (under tension) to flow from the soil to the tensiometer water reservoir or vice versa. Water pressure in the tensiometer water reservoir is measured by a piezo-electric pressure sensor positioned at the top of the tensiometer water reservoir. The back of the sensing diaphragm is vented to the atmosphere via the electrical cable, and, as a result, the tensiometer measures gauge pore-water pressure.

The electrical cable carrying the power supply and the output analog signal was connected to an external plug located in the metal box. The acceleration measurement system is based on MEMS (Micro-Electro-Mechanical-Systems) capacitive accelerometer that measures the part of gravity accelerations activated by the tilting.

Further specifications can be found in Coppola et al. (2022).

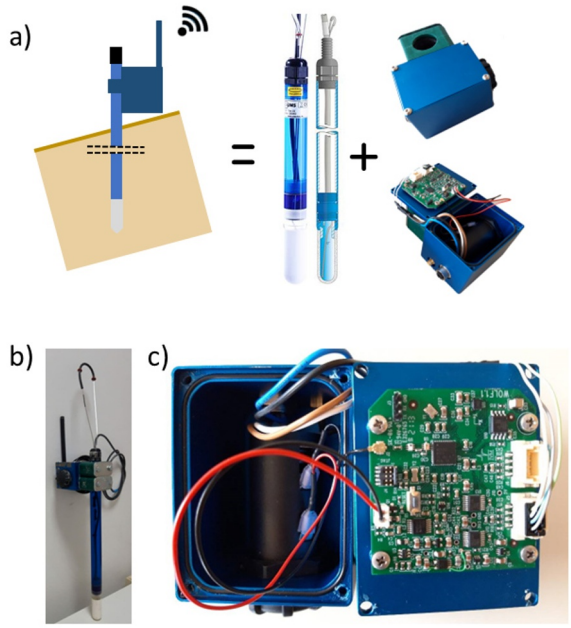

Figure 1. a) Schematic layout of the tensio-inclinometer, b) tensio-inclinometer and c) internal view of the metal box.

3. Experimental activity

3.1. Slope physical model

The slope physical model is made up of a tilting tank. It has a rectangular base (2 m long and 1.5 m wide) (Fig. 2). Due to the height of the side walls, a soil layer with a maximum height of 0.35 m may be accommodated (in the direction orthogonal to the base). The width-to-thickness ratio of the slope physical model results relatively high to minimise the effect of friction along the longitudinal boundaries. This one represents a key aspect of the experimental design, as lateral friction could hinder pre-failure deformation of the slope.

The downslope wall was made of a perforated steel sheet to maintain the soil layer in place once the tank was tilted and allow for water drainage at the same time. In addition, a geotextile was interposed between the base of the tank and the soil layer to increase the interface frictional resistance.

The tank base was supported by a steel frame with a hinge at the mid-length tank. A hydraulic actuator operated manually allowed tilting of the tank up to 45°. Three steel portals carrying each brass nozzle were positioned above the soil surface to generate nebulised rain. The nozzles have 1.19 mm wide orifice tips allowing water flow rates in the range between 0.32 to 1.95 l/min for water pressures between 0.2 and 10 bars, respectively.

The tested soil was a non-plastic, cohesionless silty sand of volcanic origin (Fig. 3). Drained isotropic-consolidated triaxial tests (not yet published) yielded a friction angle of ϕ'=33°. Permeameter laboratory tests (not yet published) yielded a saturated hydraulic conductivity of 3×10^{-7} m/s.

A motorised total station measured surface displacements.

Figure 2. Slope physical model: geometrical size.

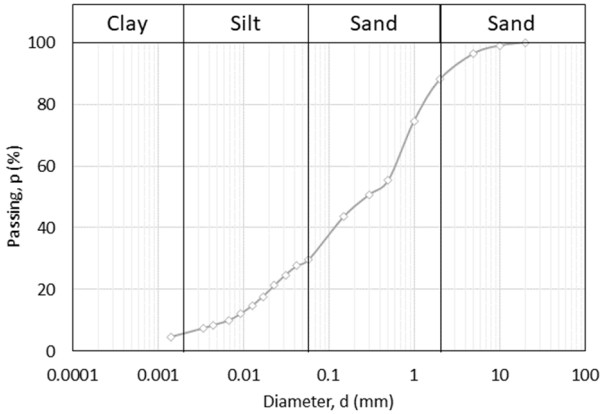

Figure 3. Grain size distribution of the tested soil.

Three tests have been carried out to explore the effect of soil bulk density and the role of vegetation. However, for the sake of brevity, only one test will be shown in the following. It was carried out on a layer thick 35 cm and prepared with dense volcanic silt. The layer was vegetated with a mixture of twelve different graminaceous plants and then tilted to 45°. The soil layer was formed by dry pluvial deposition maintaining the tank horizontally. Later, the tank was tilted, and an artificial rain of 28 mm/h was applied until global instability was observed.

3.2. Results

After the deposition, three samples were collected from the layer at different locations. The porosity of each one of them was measured. It was in-between 61% and 64%.

After the seeding phase, the layer was repeatedly wetted over a month to facilitate vegetation growth. A single sowing was sufficient to cover the entire surface. During this period, roots reached the bottom of the tank. The tank was first tilted to 36°. Three nozzles and six tensio-inclinometers were installed, as shown in Fig. 4. The tensio-inclinometers were pushed to the depths of 35, 25 and 10 cm (Fig. 4). All the tensio-inclinometers were installed with the box at the top of the shaft turned upslope, and as close as possible to the ground surface to minimise overturning moments. The devices D_{A1}, D_{B1} and D_{C1} were placed in the soil quasi-vertically while the other devices were positioned following the direction orthogonal to the slope upper surface. The tensio-inclinometers were placed in the upper portion of the slope to minimise the effect of the kinematic constraint imposed by the downslope rigid wall. Instruments and markers were placed along three lines labelled A, B and C. The motorised total station targeted four markers placed at the top of shafts pushed into the soil layer and placed closer to the tensio-inclinometers of the alignment A and C.

In this first stage of the test, rainfall was applied long enough to generate slightly positive pore-water pressures. Fig. 5a shows the evolution of tilting and suction measured by the D_{C1} device. It worth be noted that negative suction indicates positive pore-water pressure. The increase in rotation corresponds to a drop in suction.

A failure surface became visible upslope through the side surface (Fig. 5b). A rotational movement occurred along the slip surface as indicated by the device counter tilting at the end of the test (Fig. 5a). However, the rotational movement stopped, and no collapse mechanism was generated.

It is worth noticing that, due to the geometrical size of the model, the 'effective' inclination of the slope is lower than the inclination of the tank. This is because the downslope wall imposes a constraint on the kinematics of global instability, forcing the failure surface that forms parallel to the base of the tank in the upper portion of the slope to flatten mid-slope to reach the rim of the downslope wall. The 'effective' slope inclination ('overtaking angle') is approximately given by the inclination of the segment joining the bottom of the upslope wall with the top of the downslope wall. This inclination was equal to 27.5° and actually governed the global instability.

The mobilised 'effective' angle of 27.5° was lower than the critical state angle (33°) but also lower than the liquefaction 'instability' line pulled up by the lower porosity. As a result, neither liquefaction nor global instability took place.

Rainfall was then interrupted; the slope was exposed to the atmosphere. Due to the evapotranspiration fluxes acting for a week, suction reached again the value of about 4 kPa. The tank was then tilted up to 45° to raise the 'effective' (overtaking) inclination from 27.5° to 35°, i.e. greater than the friction angle of 33° to promote global instability of the slope.

Rainfall was applied again, with the same intensity. Rainwater initially infiltrated into the slope until some rainwater started to runoff. Due to the presence of the diffuse root system, local instabilities were initially inhibited. Global instability was observed about 70 min after the start of the rainfall. Fig. 6 shows the sequence of the evolution of the slope over the test.

Figg. 7, 8 and 9 show the evolution of rotation and suction recorded by the tensio-inclinometers combined with the surface displacements of the markers recorded by the total station. It is worth noticing that one of the tensio-inclinometer installed along alignment B malfunctioned. Therefore, data from this device are missing. It can be noted that rotation increases as suction decreases. A rotation increase is recorded well ahead of global instability. However, the stiffer response of the soil 'reinforced' by the root system and/or the relativity low porosity resulted in rotations in the range 1-5°. The evolution of rotations is highly consistent with the evolution of parallel-to-slope displacements. Suction paths show that global instability took place under slightly positive pore-water pressures.

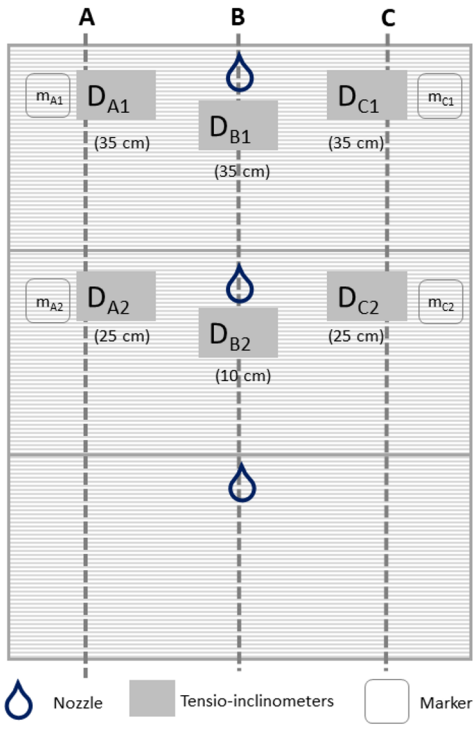

Figure 4. Position of nozzles, tensio-inclinometers and markers.

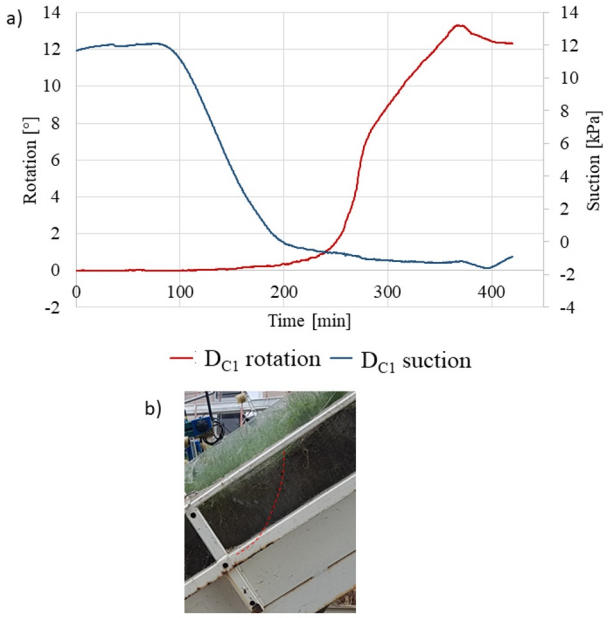

Figure 5. Measurement of rotation and suction during the first stage of the test and failure surface (from Coppola et al., 2022).

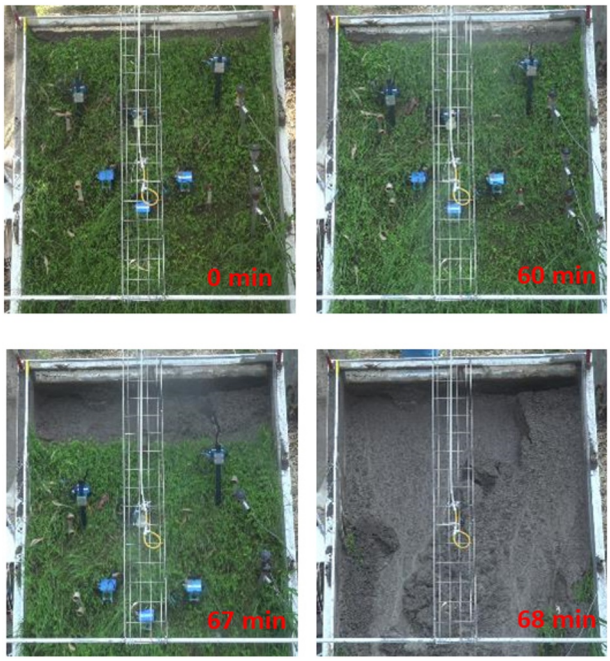

Figure 6. Images taken at different test stages (from Coppola et al., 2022).

4. Discussion

Tests in the slope physical model clearly show that the volcanic silty slope experiences suction-induced deformation due to the simulated rainfall, even considering a 35 cm thick model. The deepening of the roots is supposed to determine a stiffer response to the cover. Despite that, the suction-induced deformation is detectable well before global instability. As a result, it is possible to consider it as a potential landslide precursor, combined with rainfall and suction records. It should be underlined that the inevitable effect of the lateral boundaries tends to generate arching and, hence, hinder pre-failure deformation compared to the one that would develop in an open slope. In other words, boundary effects do not undermine the experimental results as far as the pre-failure deformation is concerned.

Suction-induced deformations are adequately captured by tilting evolution. Its measurement can hence successfully replace measurements of absolute surface displacements. These finding are relevant in designing and implementing light and effective LEWS monitoring systems because measuring the rotation of a tensiometer shaft installed in the slope (with the added benefit of suction measurement) results considerably simpler than setting a displacement monitoring system which is typically expensive and difficult to install and manage (Uchimura et al., 2015). Techniques for monitoring displacements also tend to become highly inaccurate under persistent rainfalls, which are those expected when the LEWS is in operation. In contrast, the tensio-inclinometer is expected to operate trouble-free even under adverse weather conditions.

Tilting and suction show a good synergy in detecting the soil's state prone to landslide initiation. The Suction-Tilting (ST) for the test is depicted in Fig. 10.

The pattern is characterized by a concave trend towards the suction-axis, with tilting increases driven by the downward infiltration of rainwater now sensed by the tensiometer tip. A convex trend towards the suction axis follows suction drops significantly at a depth of the tensiometer tip leading to an increasing rotation rate up to instability.

The curve inflection point could define the threshold used to issue the alarm. The inflection points occurred at times much closer to failure, 10 minutes ahead of failure. However, the failure in the slope physical model occurred in a relatively short time due to the extremely high rainfall (28 mm/h) applied to the 35 cm thick slope. In real cases, the rainfall duration triggering slope instability would be tens of hours rather than minutes (Coppola et al., 2020). A mid-time inflexion point would allow issuing a warning several hours in advance.

The test in the slope physical model also indicates the proper installation of the tensio-inclinometer. The most effective procedure appeared to be pushing the entire shaft in the layer, leaving the box near the soil ground.

5. Conclusions

The accuracy of early-warning systems for rainfall-induced shallow landslides may be significantly enhanced by monitoring precursor variables associated with the stress-strain state of the ground (in addition to the monitoring of more traditional meteorological variables). In this context, the paper has investigated whether wetting-induced instability in a special class of soils susceptible to failure upon rainfall events (i.e., high-porosity silty volcanic soils) is associated with appreciable pre-failure deformations before failure. If this is the case, the combined measurement of suction and suction-induced deformation will serve as an effective precursor variable to underpin landslide early-warning systems.

The paper first presented a tensio-inclinometer specifically developed to measure suction changes and suction-induced deformation in shallow slopes. The device was developed by mounting a MEMS accelerometer to the shaft of a conventional tensiometer. On-board electronics for data digitisation, data storage, wireless data transmission, and battery-based power supply make the device fully wireless. The tensio-inclinometer is, therefore, easy to deploy and install. Furthermore, the standing-alone tensio-inclinometer would allow designing a very flexible and adaptive monitoring system, where a small number of fixed devices is complemented by several mobile devices that can be readily deployed as needed.

The tensio-Inclinometer was then used to monitor suction and suction-induced deformation in an artificial slope subjected to artificial rainfall. It has been shown that pre-failure deformation detected via the tilting of the tensiometer shaft is an adequate landslide precursor. If recorded in combination with suction, pre-failure deformation can provide an adequate soil-based threshold. Although the interpretation of suction–tilting curves requires further investigation via field scale tests, the preliminary results presented in the paper provide a TRL3 proof-of-concept (according to European Commission, 2017) for early-warning thresholds built upon combined measurement of suction and suction-induced kinematics, possibly via the wireless and fully

deployable tensio-inclinometer. The tensio-inclinometers used in this work were relatively short and could therefore be installed at relatively shallow depths. However, it would be relatively easy to turn longer commercial tensiometers (up to 2 m) into tensio-inclinometers. These could therefore be used to monitor slopes up to two-meter thicknesses, which is the typical thickness range encountered in rainfall-induced landslides in silty volcanic slopes.

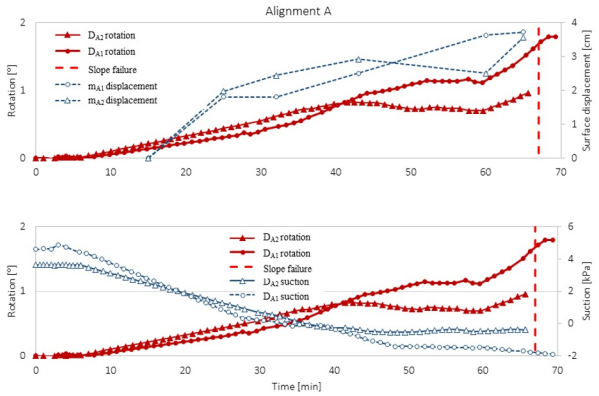

Figure 7. Rotation and comparison with markers surface displacements and simultaneous measurements of rotation and suction for the alignment A (from Coppola et al., 2022).

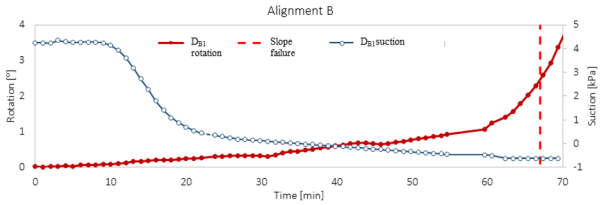

Figure 8. Simultaneous measurement of rotation and suction for the alignment B (from Coppola et al., 2022).

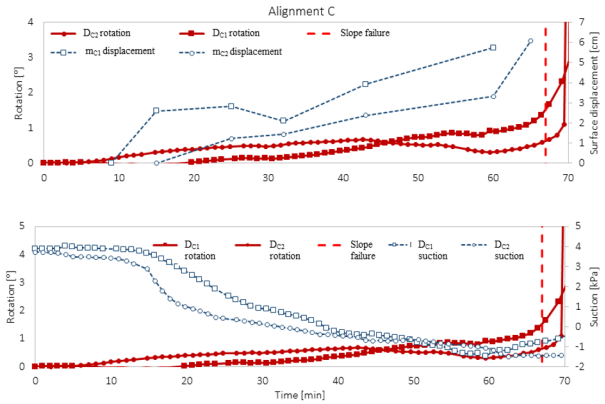

Figure 9. Rotation and comparison with markers surface displacements and simultaneous measurements of rotation and suction for the alignment C (from Coppola et al., 2022).

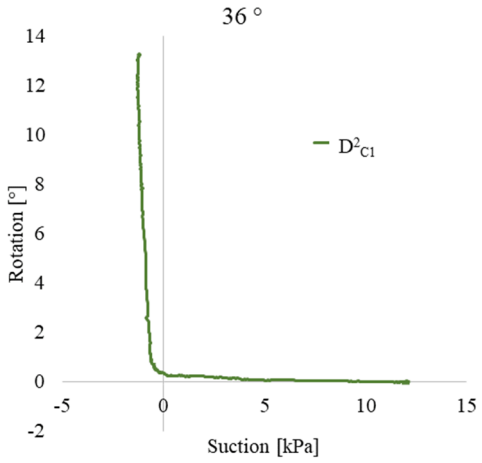

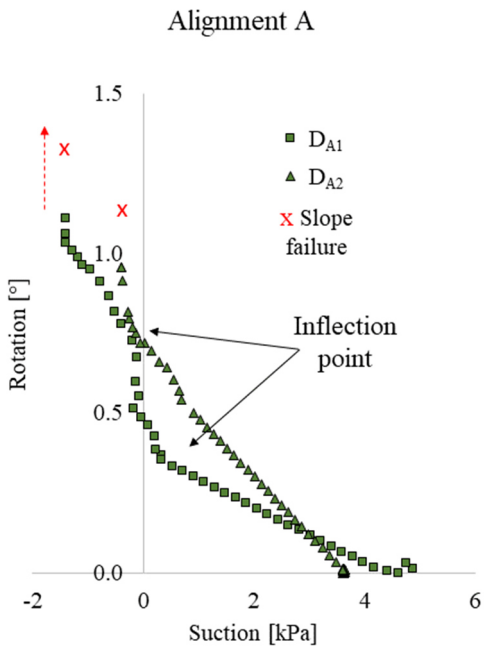

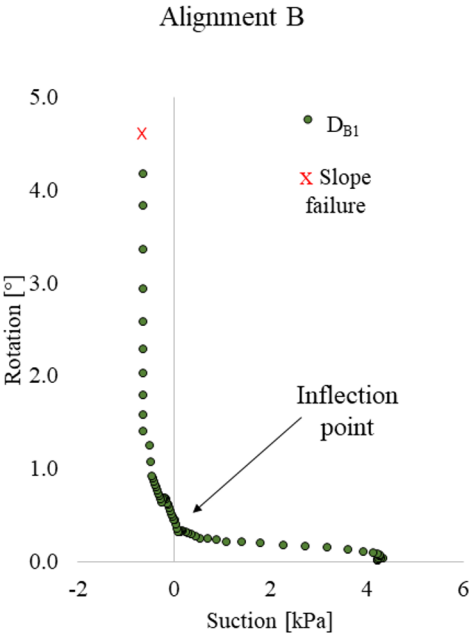

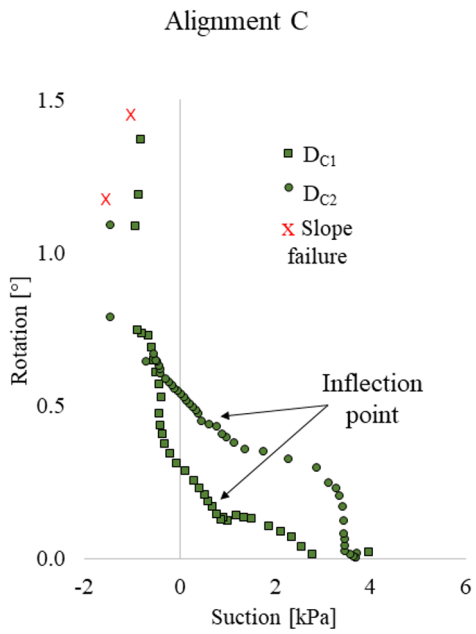

Figure 10. Rotation versus suction and warning threshold criterion (from Coppola et al., 2022).

Acknowledgements

This work was conducted within the framework of the PhD research project: "Development of an early warning system for rainfall-induced landslides based on rain gauges and tensio-inclinometer measurements" under the Programme P.O.R. – CAMPANIA FSE 2014/2020 funded by the Campania region, carried out at the PhD school of Civil Systems Engineering of the University of Naples "Federico II".

References

Alfieri L., Salamon P., Pappenberger F., Wetterhall F., Thielen J 2012.: "Operational early warning systems for water-related hazards in Europe". Environmental Science& Policy, 21, 35–49, http://dx.doi.org/10.1016/j.envsci.2012.01.008

Balzano, B., Tarantino A., and Ridley A. 2019a. "Preliminary analysis on the impacts of the rhizosphere on occurrence of rainfall-induced shallow landslides". Landslides. 1610. 1885-1901. https://doi.org/10.1007/s10346-019-01197-5

Balzano, B., Tarantino A., Nicotera M. V., Forte G., de Falco M., Santo A. 2019b.: "Building physically based models for assessing rainfall-induced shallow landslide hazard at catchment scale: case study of the Sorrento Peninsula Italy". Can. Geotech. J. 56: 1291–1303 2019 https://doi.org/10.1139/cgj-2017-0611

Barla, M.; Antolini, F. 2016: "An integrated methodology for landslides' early warning systems". Landslides, 13, 215–228. https://doi.org/10.1007/s10346-015-0563-8

Baum, R.L., and Godt, J.W. 2010: "Early warning of rainfall-induced shallow landslides and debris flows in the USA", Landslides, 7, 259–272.

Baum, R.L., Savage, W.Z., and Godt, J.W. 2008: "TRIGRS – A FORTRAN program for transient rainfall infiltration and grid-based regional slope stability analysis", vers. 2.0, U.S. Geol. Survey Open-File Rep. 424, 38.

Chleborad, A. F., Baum, R. L., Godt, J. W., & Powers, P. S. 2008. "A prototype system for forecasting landslides in the Seattle, Washington", area. Reviews in Engineering Geology, 20, 103-120.

Coppola, L., Reder, A., Rianna, G., & Pagano, L. (2020). "The role of cover thickness in the rainfall-induced landslides of Nocera Inferiore 2005". Geosciences, 10(6), 228.

Coppola, L., Reder, A., Tarantino, A., Mannara G., Pagano, L. 2022. "Pre-failure suction-induced deformation to inform early warning of shallow landslides: Proof of concept at slope model scale", Engineering Geology, Volume 309, 2022, 106834, ISSN 0013-7952, https://doi.org/10.1016/j.enggeo.2022.106834

European Commission, 2017. Horizon 2020 Work Programme 2016–2017. Available online: https://ec.europa.eu/research/participants/data/ref/h2020/other/wp/2016-2017/annexes/h2020-wp1617-annex-ga_en.pdf (accessed on 28/10/2022).

Formetta, G., Simoni, S., Godt, J.W., Lu, N., and Rigon, R. 2016: "Geomorphological control on variably saturated hillslope hydrology and slope instability". Water Resour. Res., 52, 6, 4590–4607.

Greco R., Pagano L. 2017.: "Basic features of the predictive tools of early warning systems for water-related natural hazards: examples for shallow landslides". Natural Hazards Earth System Sciences, 1712, 2213-2227, https://doi.org/10.5194/nhess-17-2213-2017

Intrieri E., Gigli G., Mugnai F., Fanti R., Casagli N. 2012: "Design and implementation of a landslide early warning system". Engineering Geology, 147–148, http://doi.org/10.1016/j.enggeo.2012.07.017

Keefer D.K., Wilson R.C., Mark R.K., Brabb E.E., Brown W.M., Ellen S.D., Harp E.L., Wieczorek G.F., Alger C.S., Zatkin R.S. 1987: "Real-time landslide warning during heavy rainfall", Science, 238, 921–925, http://doi.org/10.1126/science.238.4829.921

Orense R.P., Towhata I., Farooq K., 2003: "Investigation of failure of sandy caused by heavy rainfall". In Proceedings of the international Conference om Fast Slope Movement – Prediction and prevention for risk mitigation FSM2003 Sorrento.

Orense, R.P., Farooq, K., Towhata, I., 2004. "Deformation behavior ofs andy slopes during rain water infiltration". Soils & Foundations. 442, 15-30. https://doi.org/10.3208/sandf.44.2_15

Ortigao, J. A. R., Justi, M. G., d'Orsi, R., & Brito, H. 2001, December. Rio-Watch 2001: "the Rio de Janeiro landslide alarm system". In Proc. 14th Southeast Asian Geotechnical Conference, edited by: Ho and Li, Hong Kong, Balkema Vol. 3, pp. 237-241.

Pagano, L, Picarelli, L., Rianna, G., and Urciuoli, G. 2010: "A simple numerical procedure for timely prediction of precipitation-induced landslides in unsaturated pyroclastic soils", Landslides, 7, 273–289.

Pecoraro G., Calvello M., Piciullo L. 2019: "Monitoring strategies for local landslide early warning systems". Landslides V.16, 213–231. https://doi.org/10.1007/s10346-018-1068-z

Ponziani F., Pandolfo C., Stelluti M., Berni N., Brocca L., Moramarco T. 2012 "Assessment of rainfall thresholds and soil moisture modeling for operational hydrogeological risk prevention in the Umbria region central Italy", Landslides, 9, 229–237. http://dx.doi.org/10.1007/s10346-011-0287-3

Reder A., Rianna G., 2021: "Exploring ERA5 reanalysis potentialities for supporting landslide investigations: a test case from Campania Region Southern Italy". Landslides, 185 1909-1924. https://doi.org/10.1007/s10346-020-01610-4

Sattele M., Brundl M., Straub D., 2015: "Reliability and effectiveness of early warning systems for natural hazards: Concept and application to debris flow warning".

Reliability Engineering and System Safety 142, 192-202. http://doi.org/10.1016/j.ress.2015.05.003

Segoni S., Rosi A., Lagomarsino D., Fanti R., Casagli N., 2018: "Brief communication: Using averaged soil moisture estimates to improve the performances of a regional-scale landslide early warning system". Nat. Hazards Earth Syst. Sci., 18, 807–812. https://doi.org/10.5194/nhess-18-807-2018

Thiebes, B.; Bell, R.; Glade, T.; Jäger, S.; Mayer, J.; Anderson, M.; Holcombe, L. 2014: "Integration of a limit-equilibrium model into a landslide early warning system". Landslides, 11, 859–875. https://doi.org/10.1007/s10346-013-0416-2

Uchimura T., Towhata I., Wang L., Nishie S., Yamaguchi H., Seko I., Qiao J., 2015: "Precaution and early warning of surface failure of slopes using tilt sensors". Soils and Foundations 2015; 555: 1086–1099. https://doi.org/10.1016/j.sandf.2015.09.010

UMS GmbH last check My, the 2nd, 2021. http://library.metergroup.com/Manuals/UMS/T4_Manual.pdf

UNISDR 2006 Available at: http://www.unisdr.org/2006/ppew/info-resources/ewc3/Global-Survey-of-Early-Warning-Systems.pdf

Yang, Z., Shao, W., Qiao, J., Huang, D., Tian, H., Lei, X., & Uchimura, T. 2017. "A multi-source early warning system of MEMS based wireless monitoring for rainfall-induced landslides". Applied Sciences, 712, 1234.

Zhu, H.H.; Shi, B.; Zhang, C.C. 2017: "FBG-based monitoring of geohazards: Current status and trends". Sensors, 17, 452. https://doi.org/10.3390/s17030452